BBAA VI International Colloquium on:
Bluff Bodies Aerodynamics & Applications
Milano, Italy, July, 20-24 2008

New Consideration on Flutter Properties basing on SBS -Fundamental Flutter Mode, Similar Selberg's Formula, Torsional Divergence Instability, and New Coupled Flutter Phenomena affected by Structural Coupling

Masaru Matsumoto[*], Hisato Matsumiya[*†], Shinya Fujiwara[*], Yasuaki Ito[*‡]

[*]Department of Civil and Earth Resources Engineering, Kyoto University,
Kyotodaigaku Katsura, Nishikyo-ku, Kyoto, Japan
E-mail:matsu@brdgeng.gee.kyoto-u.ac.jp, Tel: +81-75-383-3165

[†]Central Research Institute of Electric Power Industry (2008.4~), 1646, Abiko, Abiko, Chiba, Japan

[‡]Shimizu Corporation (2007.4~), 2-3, Shibaura 1-chome, Minato-ku, Tokyo 105-8007, Japan

Keywords: step-by-step analysis, Fundamental flutter modes, Selberg's formula

1 INTRODUCTION

Authors reported that flutter characteristics, including velocity-frequency characteristic V-ω, velocity-damping characteristic V-δ, velocity-amplitude ratio characteristic V-η_0/ϕ_0, and velocity-phase difference characteristic V-Ψ, obtained by step-by-step analysis (SBSA) [1] and Complex-Eigen-Value analysis (CEVA) showed perfect agreement up to analyzed 6 digits [2]. In this paper, by using SBSA, physical meanings of coupled flutter branch of thin plate and plate-like body are discussed in relation to fundamental flutter modes. And, flutter onset velocity and branch switch characteristics are investigated basing on these two fundamental flutter modes. Furthermore, it is clarified that torsional divergence is classified into static 1DOF torsional divergence and dynamic 2 degree of freedom (DOF) torsional divergence. Moreover, similar form of Selberg's formula [3] which evaluates flutter onset velocity can be obtained basing on SBSA in torsional branch (TB) characteristics. Besides, in this study focusing on the horizontal displacement and sequential torsional displacement as structural properties, 2DOF aerodynamic coupling flutter instability affected by structural coupling between horizontal and torsional displacements have been considered in flutter analysis instead of 3DOF modes, those are vertical bending mode, torsional mode and horizontal bending mode of long span suspension bridges with truss-stiffened girder.

2 STEP-BY-STEP FLUTTER ANALYSIS

In SBSA, reported by authors [1], in which the flutter frequency in heaving branch (HB) and TB has been converged in iterative calculation, then there is some discrepancies in flutter values including damping v.s. velocity, frequency v.s. velocity characteristics, amplitude ratio v.s. velocity and phase difference v.s. velocity, between numerical results obtained by CEVA and SBSA at higher reduced velocity than flutter onset reduced velocity. Therefore, both of flutter frequency and damping have been simultaneously converged in iteration calculation in

order to resolve the difference in flutter values in two different analyses. This modified SBSA is applied in flutter analysis in the following a series of analyses described below. The brief analytical process in TB is as follows;

step1) in torsional system, torsional motion is assumed taking the damping in consideration.

$$\phi=\phi_0 e^{-\zeta'_F \omega_F t}\sin\omega_F t \tag{1}$$

step2) heaving motion is generated by torsional motion as forced vibration, with a certain amplitude ratio and phase difference.

$$\ddot{\eta}+2\zeta^*_\eta\omega^*_\eta\dot{\eta}+\omega^{*2}_\eta\eta=(\frac{\rho b^3}{m})\omega_F H^*_2\dot{\phi}+(\frac{\rho b^3}{m})\omega_F{}^2 H^*_3\phi \tag{2}$$

step3) torsional motion is also generated by heaving motion as free vibration. Finally, the flutter logarithmic damping and the flutter circular frequency are calculated with the following equations.

$$\begin{aligned}\delta_F=2\zeta_{\phi 0}\omega_{\phi 0}\frac{\pi}{\omega_F}-\pi\Omega_1 A^*_2-\pi\Omega_1\Omega_2\Big\{&A^*_1\left|H^*_2\right|(1+\zeta'^2_F)^{1/2}(\zeta'_F\sin\theta_1+\cos\theta_1)\\&+A^*_1\left|H^*_3\right|(\zeta'_F\sin\theta_2+\cos\theta_2)-A^*_4\left|H^*_2\right|(1+\zeta'^2_F)^{1/2}\sin\theta_1-A^*_4\left|H^*_3\right|\sin\theta_2\Big\}\end{aligned} \tag{3}$$

$$\begin{aligned}\omega_F=\Big[\Big\{\omega_{\phi 0}{}^2-\Omega_1\omega_F{}^2A^*_3-\Omega_1\Omega_2\omega_F{}^2\{&A^*_1\left|H^*_2\right|(1+\zeta'^2_F)^{3/2}\sin\theta_1+A^*_1\left|H^*_3\right|(1+\zeta'^2_F)\sin\theta_2\\&+A^*_4\left|H^*_2\right|(1+\zeta'^2_F)^{1/2}(\cos\theta_1-\zeta'_F\sin\theta_1)+A^*_4\left|H^*_3\right|(\cos\theta_2-\zeta'_F\sin\theta_2)\}\Big\}(1-\zeta_F{}^2)\Big]^{1/2}\end{aligned} \tag{4}$$

where, $\Omega_1=(\frac{\rho b^4}{I}),\Omega_2=\dfrac{(\frac{\rho b^2}{m})\omega_F{}^2}{\sqrt{(\zeta'^2_F\omega_F{}^2-\omega_F{}^2-2\zeta^*_\eta\zeta'_F\omega^*_\eta\omega_F+\omega^{*2}_\eta)^2+(2\zeta^*_\eta\omega^*_\eta\omega_F-2\zeta'_F\omega_F{}^2)^2}}$ (5)

step4) Then, convergence calculation associated with flutter frequency in step3 and originally assumed flutter frequency in step1, is carried out.

Then, all of flutter values obtained by this modified SBSA shows complete identical values obtained by CEVA, exceptionally branch switch, up to six digits in analyzed values. Fig.1 shows the comparison of flutter values for rectangular cylinder with *B*/*D*=20 obtained by numerical analysis, by CEVA and SBSA, and wind tunnel tests result.

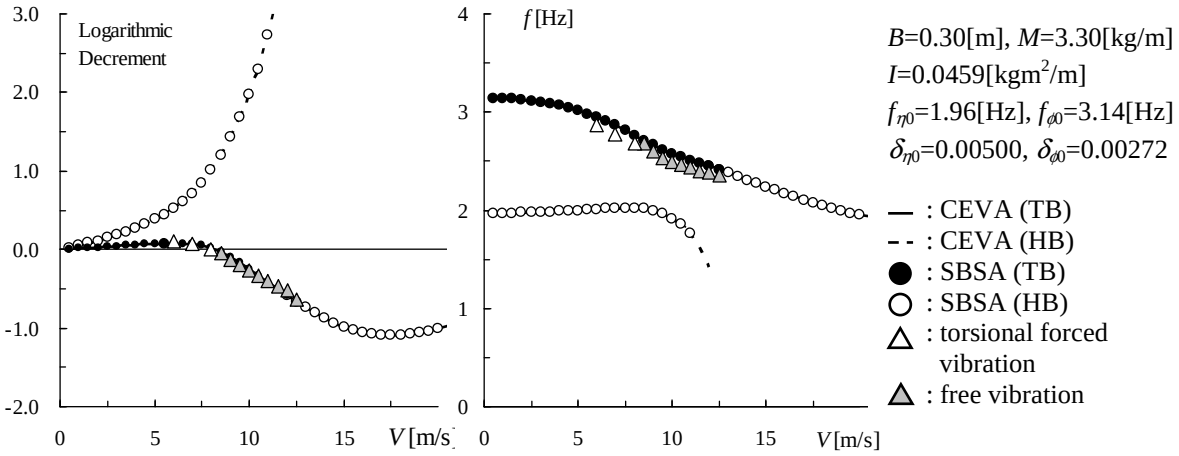

Fig.1 comparison of flutter values for rectangular cylinder with *B*/*D*=20

3 FUNDAMENTAL FLUTTER MODE

3.1 Fundamental flutter modes in torsional and heaving 2DOF coupled flutter

Torsional fundamental mode is defined as substantially torsional vibration around certain point apart from mid-chord point. In this mode, the phase difference, between torsional (noses-up positive) and heaving response (downward positive) at mid-chord point, is 0° or 180° and torsional twist center is upstream point or downward point from the mid-chord point, respectively. These fundamental modes are expressed by T_0 or T_{180}. As shown in Fig.2(a), (b), in these modes, torsional response would be excited by the pitching moment $A_1^* \dot{\eta}$ induced by relative pitching angle by $\dot{\eta}/V$, in which η is heaving displacement at mid-chord point.

On the other hand, heaving fundamental mode is defined as prominent heaving response induced by lift generated by slight pitching angle in quasi-steady sense with -90° or 90° as phase lag of heaving to torsional displacements. These two fundamental modes correspond to $dC_L/d\alpha>0$ or $dC_L/d\alpha<0$ and are expressed by H_{-90} or H_{90}, respectively. In heaving mode, heaving response is excited by lift force $H_3^* \phi$ by slight torsional response ϕ in the quasi-steady state. H_{-90} and H_{90} are illustrated as Fig.2(c), (d).

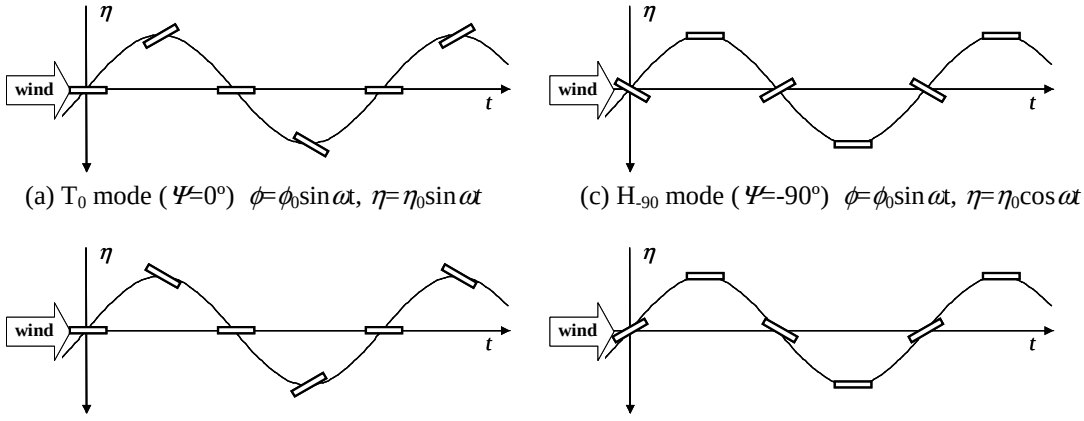

(a) T_0 mode (Ψ=0º) $\phi=\phi_0\sin\omega t$, $\eta=\eta_0\sin\omega t$

(c) H_{-90} mode (Ψ=-90º) $\phi=\phi_0\sin\omega t$, $\eta=\eta_0\cos\omega t$

(b) T_{180} mode (Ψ=180º) $\phi=\phi_0\sin\omega t$, $\eta=-\eta_0\sin\omega t$

(d) H_{90} mode (Ψ=90º) $\phi=\phi_0\sin\omega t$, $\eta=-\eta_0\cos\omega t$

Fig.2 Fundamental flutter modes in torsional and heaving 2DOF coupled flutter

By taking into account of fundamental mode definition, the flutter mode in coupled flutter can be resolved into two fundamental modes by using phase difference Ψ, in which Ψ is defined as heaving lag to torsional response as Eq. (6). And the contribution of each fundamental mode is expressed by Eq. (7).

$$\phi=\phi_0\sin\omega t,\ \eta=\eta_0\sin(\omega t-\Psi) \tag{6}$$

$$\begin{aligned} &T_{180}=-\cos\Psi,\ H_{90}=\sin\Psi\ (90^\circ\le\Psi\le180^\circ)\\ &T_0=\cos\Psi,\ H_{90}=\sin\Psi\ (0^\circ\le\Psi\le90^\circ)\\ &T_0=\cos\Psi,\ H_{-90}=-\sin\Psi\ (-90^\circ\le\Psi\le0^\circ)\\ &T_{180}=-\cos\Psi,\ H_{-90}=-\sin\Psi\ (-180^\circ\le\Psi\le-90^\circ) \end{aligned} \tag{7}$$

3.2 Relation between flutter branch and fundamental flutter modes

The flutter fundamental modes are closely related to flutter branch of SBSA explained as follows [2].

Torsional branch

Step1: torsional oscillation.

$$\phi(t)=\phi_0 e^{i\omega_\phi t} e^{-\zeta_\phi \omega_\phi t} \tag{8}$$

Step2: Unsteady lifts, $H_2^* \dot{\phi}$ and $H_3^* \phi$, act on η system as forced vibration- forces. Then, η response with ω_ϕ can be excited. In this step, amplitude ratio and phase difference between heaving and torsional response can be characterized.

Step3: Unsteady moment, $A_1^* \dot{\eta}$ and $A_4^* \eta$, generated by heaving response at step2, act on torsional system as self excited moments, then flutter frequency $\omega_F(=\omega_\phi)$ and flutter damping $\delta_F(=\delta_\phi)$ can be characterized, if δ_ϕ and ω_ϕ in step1 are identical to those in step3. In which, $H_1^* \dot{\eta}$ is self excited pitching moment induced by $\dot{\eta}$, therefore, the torsional response should correspond fundamental flutter modes T_0 and T_{180}.

Heaving Branch

Step1: heaving oscillation.

$$\eta(t)=\eta_0 e^{i\omega_\eta t} e^{-\zeta_\eta \omega_\eta t} \tag{9}$$

Step2: Unsteady moments, $A_1^* \dot{\eta}$ and $A_4^* \eta$ act on torsional system as forced vibration-forces. Then, ϕ response with ω_η can be excited. In this step, amplitude ratio and phase difference between heaving and torsional response can be characterized.

Step3: Unsteady lift, $H_2^* \dot{\phi}$ and $H_3^* \phi$, generated by torsional response at step2, act on heaving system as self excited lift forces, then flutter frequency $\omega_F(=\omega_\eta)$ and flutter damping $\delta_F(=\delta_\eta)$can be characterized, if δ_η and ω_η at step1are identical to those at step3. In which, $H_3^* \phi$ is unsteady lift induced by relative pitching angle due to torsional response ϕ, and heaving response induced by self excited action of $H_3^* \phi$ should correspond the flutter fundamental modes H_{-90} and H_{90}.

Thus it is verified that in TB, T_0 and T_{180} are classified to self-excite term on the other hand H_{-90} and H_{90} to forced term. As contrast, in HB, H_{-90} and H_{90} are subjected to self-excited term and T_0 and T_{180} to forced term.

3.3 Flutter onset velocity branch switch related to fundamental flutter modes

By using Eq. (7) and phase difference Ψ, flutter modes are resolved as shown in Fig.3. As shown, for the case frequency ratio of $f_{\phi 0}/f_{\eta 0}$=1.3, flutter onsets in TB at V=9.6 [m/s] and the flutter major branch switches from TB to HB at V=11.1 [m/s]. Comparing these characteristics, velocities and the flutter fundamental modes, it is clarified that for TB when the self excited term T_0 (=cos Ψ) becomes large, flutter might onset. Furthermore, when the self-excited-term H_{-90} (=-sin Ψ) becomes large, branch switch seems to occur. However, there remains some questions in TB, at the maximum value of T_0 does not correspond the flutter onset velocity. On the other hand, when H_{-90} becomes large enough in HB, the branch switch from TB to HB seems to occur. Therefore, more details should be studied, taking into account the flutter fundamental modes. And these give us some hints about the physical generation mechanism and branch switch of coupled flutter.

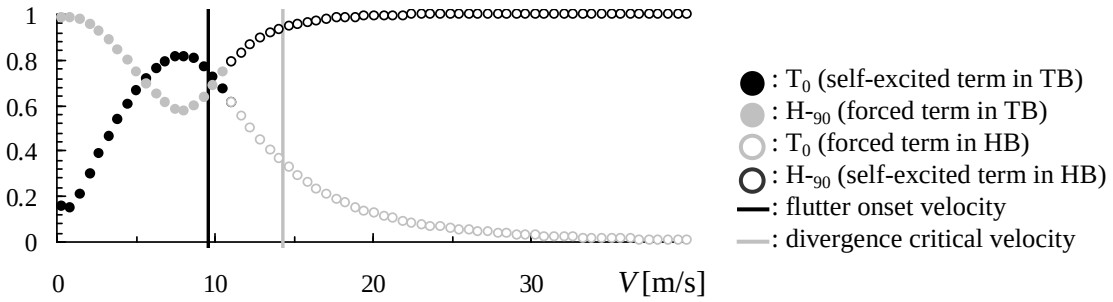

Fig.3: Flutter major mode in thin plate frequency ratio 1.3

4 SIMILAR FORMULA WITH SELBERG'S FORMULA TO PREDICT THE FLUTTER ONSET VELOCITY OF THIN PLATE

The following lines show discussion about Selberg's formula [3] which is a well-known evaluation formula of flutter onset velocity for thin plate, as described Eq. (10).

$$V_F = 3.71 \cdot f_{\phi 0} \cdot (2b) \sqrt{\frac{\sqrt{mI}}{\rho (2b)^3} \left\{ 1 - \left(\frac{f_{\eta 0}}{f_{\phi 0}} \right)^2 \right\}} \tag{10}$$

Then, authors investigate the formula to predict the flutter onset velocity by using SBSA. It is clarified that flutter onset velocity is almost agreed to crossing point of ω_η-V diagram and ω_ϕ-V diagram of TB, as shown in Fig.4. Then, the following assumptions are used.
Assumption1: Quasi-steady state; $F(k)$=1, and $G(k)$=0, where $C(k)$=$F(k)$-$iG(k)$.
Assumption2: Flutter occurs, when crossing point of ω_η-V diagram and ω_ϕ-V diagram.
Assumption3: ω_η=$\omega_{\eta 0}$ at any velocity and ω_ϕ in 2DOF can be approximately expressed by ω_ϕ in 1DOF.

Torsional 1DOF frequency is described as Eq. (11).

$$\omega'_\phi = \sqrt{{\omega_{\phi 0}}^2 - (\frac{\rho b^4}{I}) {\omega_\phi}^2 A_3^*} \tag{11}$$

Then, aerodynamic derivatives are described as Eq. (12).

$$A_3^* = \frac{\pi}{k} \left(\frac{F(k)}{k} + \frac{G(k)}{2} \right) = \frac{\pi}{k^2} = \frac{V^2 \pi}{(b\omega_\phi)^2} \tag{12}$$

Using assumption of $F(k)$=1, $G(k)$=0 (Assumption1), torsional 1DOF frequency is described as Eq. (13).

$$\omega_\phi^* = \sqrt{{\omega_{\phi 0}}^2 \Big/ (1 + \frac{\rho b^4}{I} \cdot \frac{\pi}{k^2})} \tag{13}$$

When flutter occurs, using ω_F=ω_η=ω_ϕ (Assumption2) and ω_η=$\omega_{\eta 0}$ and ω_ϕ (2DOF) =ω_ϕ (1DOF)(Assumption3), the following equation can be derived. Where, k=$b\omega_F/V$=$b\omega_\eta/V$ =$b\omega_{\eta 0}/V$ (because of TB).

$$V_r = f_{\phi 0} \sqrt{\frac{4\pi I}{\rho b^4} \left\{ 1 - \left(\frac{f_{\eta 0}}{f_{\phi 0}} \right)^2 \right\}} \tag{14}$$

Eq. (14) is transformed the following equation.

$$V_F = \sqrt{\frac{8\pi\sqrt{I}}{b\sqrt{m}}} \cdot f_{\phi 0} \cdot 2b \sqrt{\frac{\sqrt{mI}}{\rho(2b)^3}\left\{1-\left(\frac{f_{\eta 0}}{f_{\phi 0}}\right)^2\right\}} \tag{15}$$

Eq. (15) is similar to Selberg's formula as described Eq. (10), and coefficient of Eq. (15) is calculated as follows. Eq. (16) and Eq. (17), relationships between m and I in thin plate, can be obtained.

$$I = \int_A \rho_s r^2 dA = \int_A \rho_s (y^2+z^2) dA = \iint_{y\ z} \rho_s (y^2+z^2) dydz = \rho_s \left(\frac{4bd^3}{3} + \frac{4b^3 d}{3}\right) \tag{16}$$

$$I = \lim_{d\to 0}(4\rho_s bd)\left(\frac{1}{3}d^2 + \frac{1}{3}b^2\right) \cong \frac{1}{3}mb^2 \tag{17}$$

Relationships between m and I in thin plate are described as $I=mb^2/3$, and Eq. (15) can be modified like Selberg's Form as follows;

$$V_F = 3.81 \cdot f_{\phi 0} \cdot (2b) \sqrt{\frac{\sqrt{mI}}{\rho(2b)^3}\left\{1-\left(\frac{f_{\eta 0}}{f_{\phi 0}}\right)^2\right\}} \tag{18}$$

As shown in Fig.5, the flutter onset velocity of thin plate obtained by CEVA or SBSA, Selberg's formula, and Eq. (18) are compared for various frequency ratios. From this figures, flutter onset velocity obtained by Eq. (18) fairly well agrees to that obtained by SBSA as well as Selberg's formula.

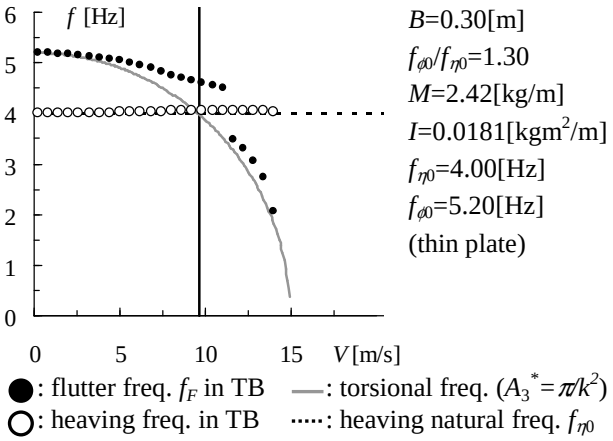

Fig.4: Frequency characteristics in TB

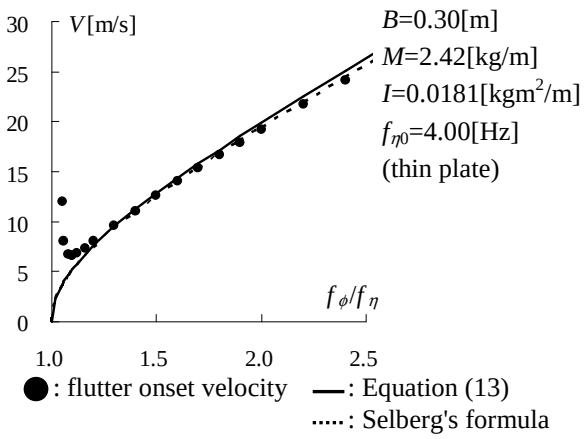

Fig.5: Comparison with flutter onset velocity

5 TORSIONAL DIVERGENCE

Torsional divergence could occur when restoring force become smaller than pitching moment force in static state. On the other hand, for dynamic system, when the torsional rigidity becomes zero due to aerodynamic unsteady pitching moment, divergence occurs. Therefore, by using SBSA, static divergence and dynamic torsional divergence can be easily studied. Torsional divergences are classified into following three different types.

(a) 1DOF divergence: Torsional rigidity is zero at Step1 of TB.

$$\omega_\phi^2 = \omega_{\phi 0}^2 - (\rho b^4 / I)\omega_\phi^2 A_3^* = 0 \tag{19}$$

In quasi-steady state ($A_3^*=2C_M'/k^2$), critical velocity is identical to static one as Eq. (20).

$$V_{cr}=\sqrt{\frac{2k_{\phi 0}}{\rho B^2 C_M^{'}}} \tag{20}$$

Where, k is reduced frequency ($k=b\omega/V$), $k_{\phi 0}$ is structural torsional rigidity at V=0 [m/s] and $C_M^{'}$ is slope of pitching moment coefficient.

(b) 2DOF dynamic divergence: Torsional rigidity is zero at Step3 of TB.

$$\omega_F^2=\omega_{\phi 0}^2-(\rho b^3/I)\omega_F^2\left\{bA_3^*-A_4^*(\eta_0/\phi_0)(\cos\Psi-\zeta_F\sin\Psi)-A_1^*(\eta_0/\phi_0)(\zeta_F^2+1)\sin\Psi\right\}=0 \tag{21}$$

(c) 1DOF dynamic divergence: Torsional rigidity is zero at step2 of HB.

$$\omega_\phi^{*2}=\omega_{\phi 0}^2-(\rho b^4/I)\omega_F^2 A_3^*=0 \tag{22}$$

These three different divergence critical velocities of thin plate in frequency ratio $f_{\phi 0}/f_{\eta 0}$=1.3 are indicated on V-f diagram as shown in Fig.6. Measured torsional divergence critical velocities of rectangular cylinder with B/D=20 under three different test conditions are compared with calculated results from Eq. (20) in Table1. Taking into account of velocity pitch is 0.5 [m/s] in this test, fairy good agreement can be seen. On the other hand, 2DOF torsional divergence is observed in the test of torsional free-vibration under heaving forced-vibration system.

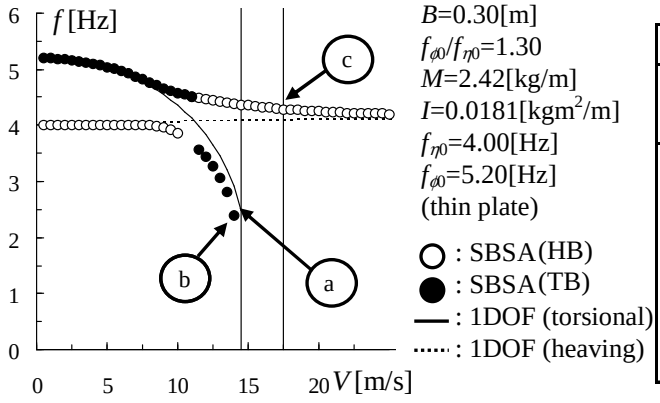

Fig.6: Three types of torsional divergence

Divergence velocity	case1	case2	case3
V_{cr} [m/s] (measured)	13.0	12.5	19.5
V_{cr} [m/s] (calculated)	14.0	14.0	19.0
m [kg/m]	3.30	2.55	4.52
I [kgm^2/m]	0.0459	0.0538	0.1162
$f_{\eta 0}$ [Hz]	1.96	2.16	2.28
$f_{\phi 0}$ [Hz]	3.14	2.956	2.77
$\delta_{\eta 0}$	0.005	0.192	0.113
$\delta_{\phi 0}$	0.003	0.179	0.058

Table1: Comparison with divergence velocity

6 2DOF COUPLED FLUTTER AFFECTED BY STRUCTURAL COUPLING OF FULL ELASTIC SUSPENSION BRIDGE WITH TRUSS-STIFFENED GIRDER(CASE OF AKASHI STRAIT BRIDGE)

Recently coupled flutter instability has been analyzed in 3DOF, that is vertical displacement η (heaving displacement), horizontal displacement ξ, and torsional displacement ϕ, analysis, instead of conventional 2DOF (η, ϕ) analysis [1]. The background of 3DOF analysis stands on the experimental results on flutter characteristics of Akashi Strait Bridge elastic full-scale model (AFM, 1/100 scale, 40m total span length) as shown in Photo 1. It has been reported that damping-velocity characteristics could not always be explained by conventional 2DOF flutter analysis [4]. 3DOF flutter analysis additionally taking into account of horizontal motion and aerodynamic forces caused by horizontal motion of bridge girder, can show better fitting to test results as shown in Fig.7 [5]. However, there are some questions

why 3DOF flutter analysis can better fit to test results, even though the aerodynamic derivatives associated to horizontal motion ξ is much smaller than the other derivatives associated to heaving η, and torsional motion ϕ as shown in Fig.8. Furthermore, looking the video film of flutter characteristics of AFM, flutter mode is significantly similar to those in 2DOF system of flat rectangular cylinder with B/D=20 (B: chord length, D: depth). In consequence, flutter of AFM could be conventional 2 DOF coupled flutter, and the discrepancy of flutter onset velocity between test results and analytical results could be caused by another reason. Therefore, in this study, focusing on the horizontal displacement and sequential torsional displacement, 2DOF aerodynamic coupling and structural coupling between horizontal and torsional displacements have been considered in flutter analysis.

Photo1: Akashi Full-scale Model, 1/100 scale, 40m total span length (courtesy of Honshu-Shikoku)

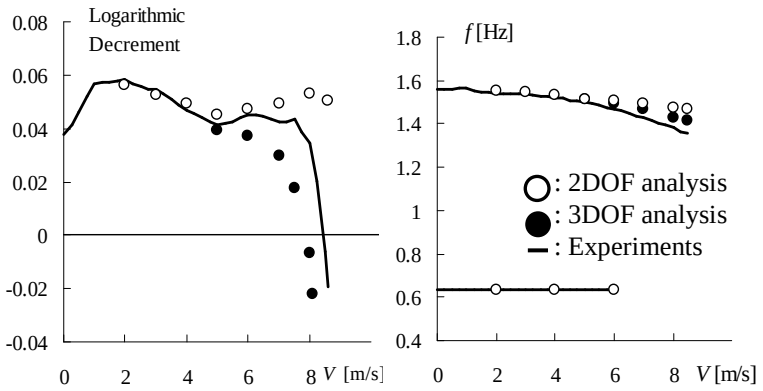

Fig.7: Results of analyses and experiments at AFM (Normal girder) [2]

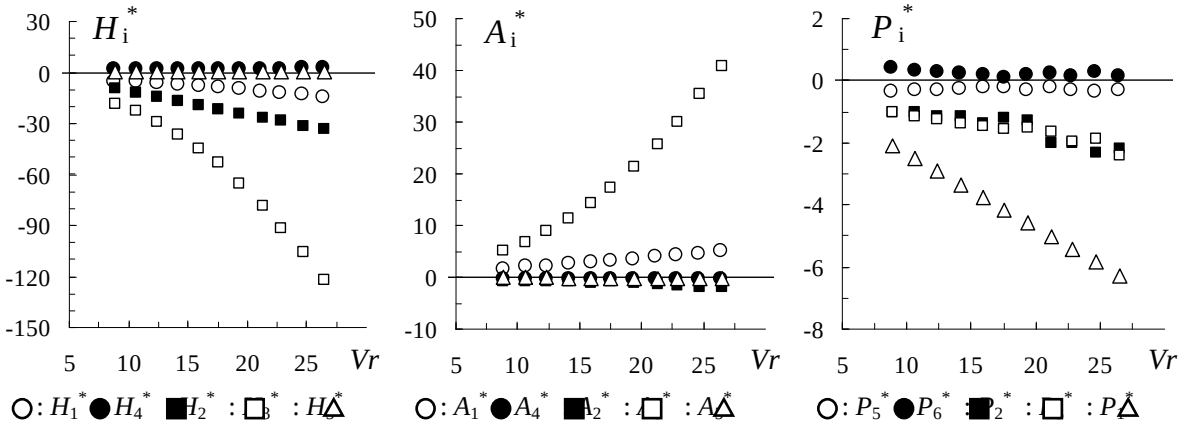

Fig.8: Aerodynamic derivatives at Akashi Strait Bridge girder (Modified, angle of attack = 0 [deg.])

By using the aerodynamic derivatives, H_i^*, A_i^* and P_i^* (i=1~6) the heaving, torsional and horizontal 3DOF differential equations are expressed as follows [6];

$$m\ddot{\eta}+C_\eta\dot{\eta}+k_\eta\eta=\frac{1}{2}\rho V^2(2b)\left[kH_1^*\frac{\dot{\eta}}{V}+kH_2^*\frac{b\dot{\phi}}{V}+k^2H_3^*\phi+k^2H_4^*\frac{\eta}{b}+kH_5^*\frac{\dot{\xi}}{V}\right] \quad (23)$$

$$I\ddot{\phi}+C_\phi\dot{\phi}+k_\phi\phi=\frac{1}{2}\rho V^2(2b^2)\left[kA_1^*\frac{\dot{\eta}}{V}+kA_2^*\frac{b\dot{\phi}}{V}+k^2A_3^*\phi+k^2A_4^*\frac{\eta}{b}+kA_5^*\frac{\dot{\xi}}{V}\right] \quad (24)$$

$$m\ddot{\xi}+C_\xi\dot{\xi}+k_\xi\xi=\frac{1}{2}\rho V^2(2b)\left[kP_1^*\frac{\dot{\xi}}{V}+kP_2^*\frac{b\dot{\phi}}{V}+k^2P_3^*\phi+kP_5^*\frac{\dot{\eta}}{V}+k^2P_6^*\frac{\eta}{b}\right] \quad (25)$$

Where η, ϕ and ξ are the heaving, torsional and horizontal displacements, m and I are the mass and mass inertia per unit length, C_η, C_ϕ and C_ξ are the damping coefficients, k_η, k_ϕ and

k_ξ are stiffness, ρ is the air density, b is the half chord length, k is the reduced frequency ($=b\omega_F/V$), ω_F is the flutter circular frequency and V is the wind velocity.

To solve the 3DOF equations, 2DOF step-by-step analysis (SBSA) [1], which has many advantages [2], should be expanded to 3DOF. Then authors propose the 3DOF SBSA method and results of this method show complete agreement with those of 3DOF Complex-Eigen-Value analysis, even though they have different branch definition. As an example, TB (in general, flutter onset mode) of 3DOF SBSA method is conducted as follows. Firstly, in torsional system, torsional motion ($\phi=\phi_0 e^{\lambda t}$, $\lambda=-\zeta_F\omega_F+i\omega_F$) is assumed in Step1. Secondly, in heaving and horizontal system, both motions are generated by torsional motion, as forced vibration in Step2. Then, by solving simultaneous equations of heaving and horizontal system, amplitude ratio η_0/ϕ_0, ξ_0/ϕ_0 and phase difference $\Psi_{\eta\phi}$, $\Psi_{\xi\phi}$ are calculated from this Step2. As Step3, in torsional system, torsional motion is also characterized by heaving and horizontal motion, which has a certain amplitude ratio and a certain phase difference, as free vibration. From this step, the flutter damping and the flutter frequency are calculated from Eq. (26) and (22). Then, convergence calculation, between calculated flutter frequency and damping in Step3 and assumed flutter frequency and damping in Step1, is carried out.

$$\begin{aligned}\zeta_F = [&2\zeta_{\phi 0}\omega_{\phi 0} + (\rho b^3/I)\omega_F\{-bA_2^* + A_4^*(\eta_0/\phi_0)\sin\Psi_{\eta\phi} \\ &- A_1^*(\eta_0/\phi_0)(\zeta_F\sin\Psi_{\eta\phi}+\cos\Psi_{\eta\phi}) - A_5^*(\xi_0/\phi_0)(\zeta_F\sin\Psi_{\xi\phi}+\cos\Psi_{\xi\phi})\}]/2\omega_F\end{aligned} \tag{26}$$

$$\begin{aligned}\omega_F = [&\omega_{\phi 0}^2 + (\rho b^3/I)\omega_F^2\{-bA_3^* - A_4^*(\eta_0/\phi_0)(\cos\Psi_{\eta\phi} - \zeta_F\sin\Psi_{\eta\phi}) \\ &- A_1^*(\eta_0/\phi_0)(\zeta_F^2+1)\sin\Psi_{\eta\phi} - A_5^*(\xi_0/\phi_0)(\zeta_F^2+1)\sin\Psi_{\xi\phi}\}]^{1/2}\end{aligned} \tag{27}$$

Similarly, in HB and horizontal branch, the flutter damping and the flutter frequency can be derived by linear summation of each aerodynamic derivative. Therefore, the effects of various aerodynamic derivatives can be clarified.

As described before, previous studies pointed out the definite role of 3DOF on coupled flutter. However, looking at video film, when flutter occurs at prototype wind velocity of 93 [m/s], flutter mode which looks like heaving and torsional 2DOF vibrating mode is observed. In this flutter mode, torsional mode is predominant and torsional fundamental mode T_0 (phase difference $\Psi_{\eta\phi}$=0 [deg.]) plays important and major role for flutter excitation at flutter onset [7]. Furthermore, as shown in Fig.9, there are almost the same results or significantly small differences between the results obtained by 2DOF and 3DOF two-dimensional flutter analyses by using flutter derivatives of Akashi Strait Bridge girder (see Fig.8).

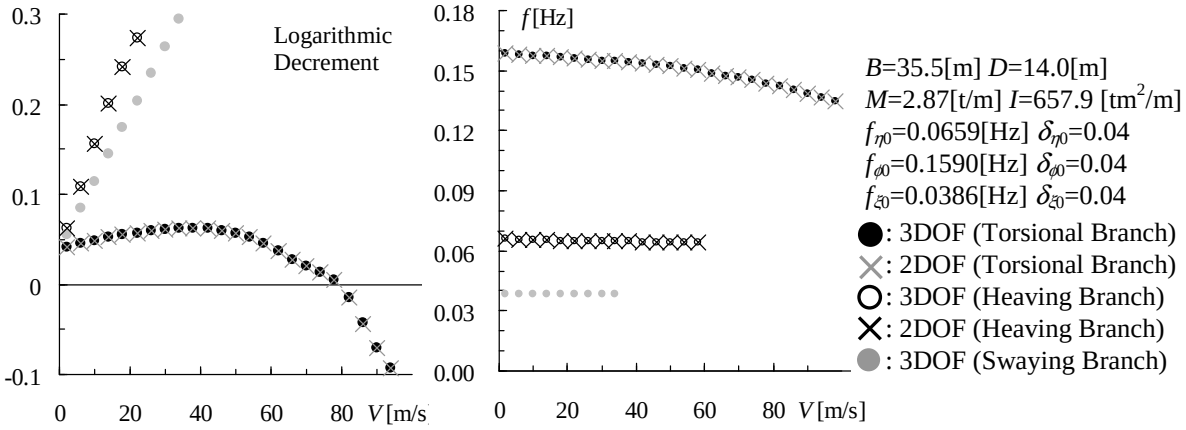

Fig.9: Comparison with results of 3DOF and 2DOF SBSA (1st sym. modes, angle of attack = 0 [deg.])

Looking at static displacement characteristics as shown in Fig.10 (a), (b), when wind velocity increases, static horizontal displacement $\xi_s(V)$ gradually increases. And static torsional displacement $\phi_s(V)$ is simultaneously induced by this horizontal displacement $\xi_s(V)$. This horizontal displacement $\xi_s(V)$ is caused by drag force *Drag*. Therefore, static torsional displacement $\phi_s(V)$ due to horizontal displacement $\xi_s(V)$ can be thought to be linear relation to drag force *Drag* as shown in Fig.10(c). In this figure, drag force *Drag* is calculated from Eq. (28) by using drag force coefficient C_D. This *Drag*-$\phi_s(V)$ characteristics should be substantially structural feature as structural coupling between horizontal displacement ξ, and torsional displacement ϕ of this AFM, only influenced by drag force.

$$Drag = \frac{1}{2}\rho V^2 D C_D \tag{28}$$

By the influence of this structural coupling characteristics, additional torsional displacement ϕ^* is generated by the change of drag force. While torsional response ϕ surely changes the drag force from quasi-steady base, therefore, the additional pitching moment term $M^*(\phi^*)$ induced by additional torsional displacement ϕ^* should be added in torsional differential equation as follows;

$$\begin{aligned} m\ddot{\eta}+C_\eta\dot{\eta}+k_\eta\eta &= \frac{1}{2}\rho V^2(2b)\left[kH_1^*\frac{\dot{\eta}}{V}+kH_2^*\frac{b\dot{\phi}}{V}+k^2H_3^*\phi+k^2H_4^*\frac{\eta}{b}\right] \\ I\ddot{\phi}+C_\phi\dot{\phi}+k_\phi\phi &= \frac{1}{2}\rho V^2(2b^2)\left[kA_1^*\frac{\dot{\eta}}{V}+kA_2^*\frac{b\dot{\phi}}{V}+k^2A_3^*\phi+k^2A_4^*\frac{\eta}{b}\right]+M^*(\phi^*) \end{aligned} \tag{29}$$

When torsional displacement is ϕ, variation of drag force $Drag(\phi)$ is described as Eq.(30) from quasi-steady state.

$$Drag(\phi) = \frac{1}{2}\rho V^2 D\frac{dC_D}{d\alpha}\phi \tag{30}$$

Taking into account of the relationship diagram between drag force *Drag* and torsional displacement $\phi_s(V)$, additional torsional displacement ϕ^* caused by structural coupling is calculated by the following.

$$\phi^* = -0.0148\times Drag(\phi) \tag{31}$$

Where coefficient (-0.0148) is obtained from structural property as shown in Fig.10 (c). Finally, additional pitching moment term $M^*(\phi^*)$ is considered as the elastic force.

$$M^*(\phi^*) = k_\phi\phi^* = -0.0074\times\rho V^2 D\frac{dC_D}{d\alpha}\omega_{\phi 0}^2\phi \tag{32}$$

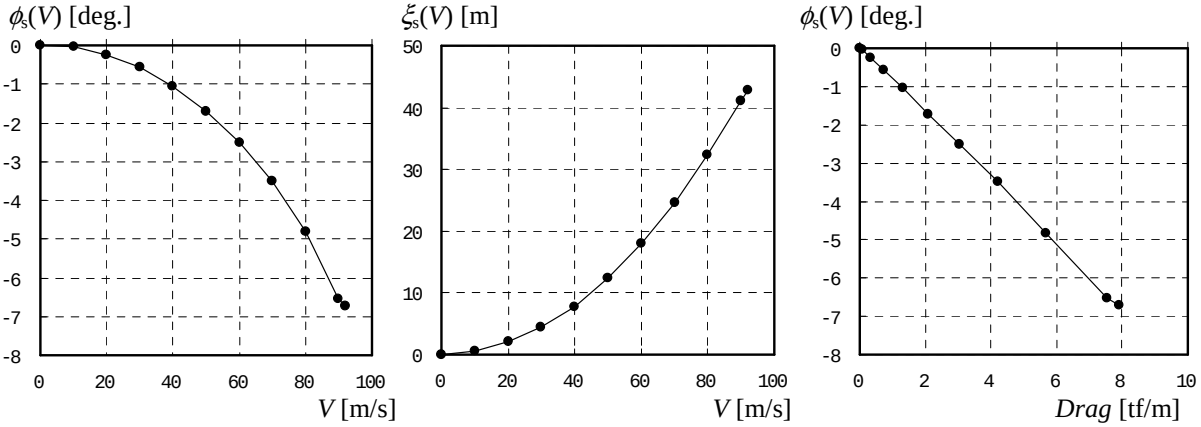

(a): Torsional displacement $\phi_s(V)$ (b): Horizontal displacement $\xi_s(V)$ (c): *Drag*-$\phi_s(V)$ relation

Fig.10 Static displacement characteristics at middle point of AFM (angle of attack = 0 [deg.])

As shown in Eq. (29) and (32), additional torsional displacement ϕ^* possess the effect to decrease torsional rigidity. Then, by using the aerodynamic derivatives of Akashi Strait Bridge girder at angle of attack = 0 [deg.] or -6 [deg.], 2DOF SBSA is conducted. The numerical results on velocity-damping (V-δ) diagram and velocity-frequency (V-ω) diagram obtained by Eq. (29) are compared with test results [2] in Fig.11 (a), (b). As shown, both results show good agreement. In particular, at near and after flutter onset, rapid decreasing characteristics of damping as velocity increases, can be well calculated by using Eq. (29). In conclusion, the author would like to emphasize that as far as the coupled flutter of AFM should not be 3DOF coupled flutter from aerodynamic point of views, but aerodynamically 2DOF coupled flutter strongly affected by structural coupling feature between horizontal displacement and torsional response. In this study, only first symmetric torsional and heaving vibration modes are considered. As future works, flutter analysis should be conducted, by taking into account higher vibration modes and the variation of static pitching angle along span axis.

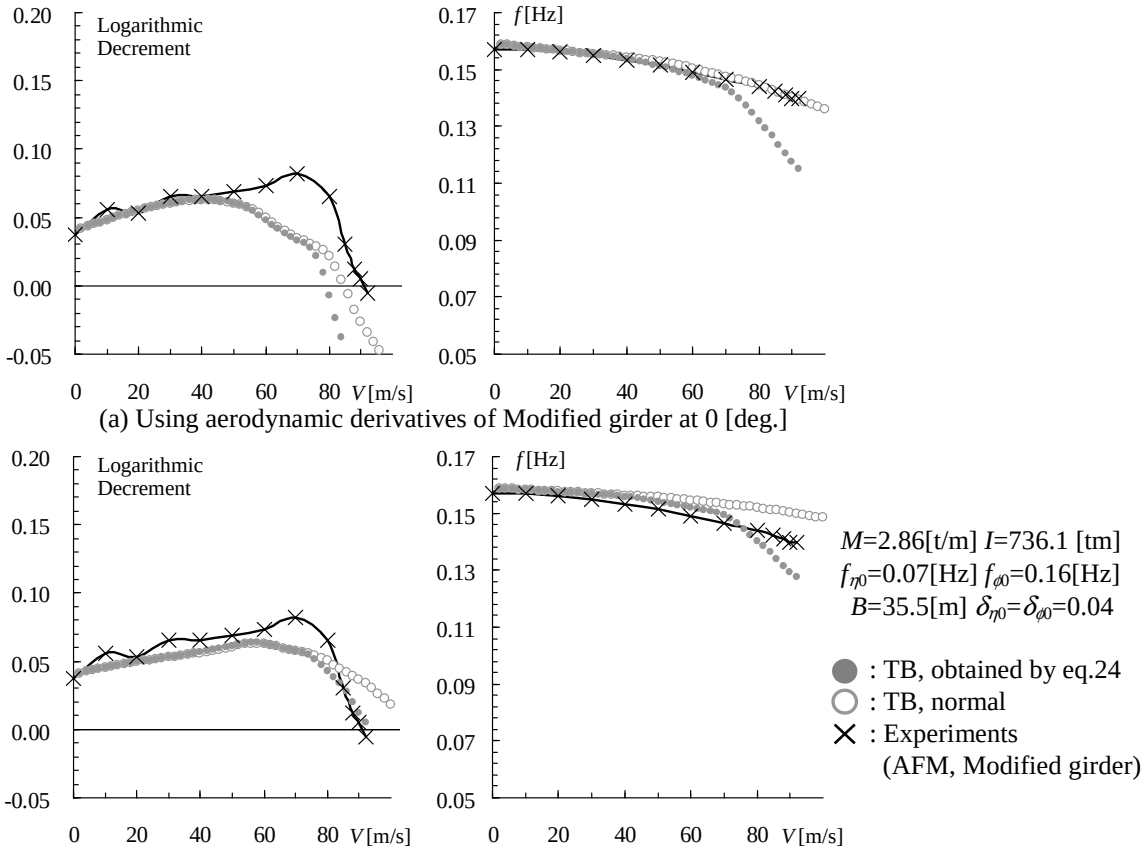

(a) Using aerodynamic derivatives of Modified girder at 0 [deg.]

(b) Using aerodynamic derivatives of Modified girder at -6 [deg.]

Fig.11: results of 2DOF (1st symmetric torsional and heaving vibration modes) SBSA with structural coupling

7 CONCLUSION

By using fundamental flutter modes, flutter modes can be resolved into torsional mode T_0 or T_{180} and heaving mode H_{-90} or H_{90}. As far as thin plate, from the point of view of self excited term, T_0 mode and H_{-90} mode play major roles in TB and HB, respectively. For flutter onset in TB, T_0 mode is essential mode, on the other hand, branch switch might be encourage

mainly by H_{-90} mode. Basing on TB characteristics flutter onset, significantly similar formula to Selberg's formula can be provided. Finally, three different torsional divergence velocities are shown by using SBSA. The coupled flutter of Full-Scale Model of Akashi-Strait Bridge can be characterized by aerodynamically conventional 2DOF (η, ϕ) coupling and structural coupling between horizontal displacement and torsional motion. Simplified analytical model developed in this study fairly well explains flutter characteristic obtained by wind tunnel tests. The authors understand that coupled flutter of plate-like structures including truss-stiffened bridge girder, flat box bridge girder and so on, would be mostly characterized by 2DOF (η, ϕ) coupling. Of course, particular section, of which aerodynamic derivatives associated to horizontal motion would be compatibly larger than those associated to heaving and torsional motion, would show 3DOF coupled flutter.

Finally, authors would like to acknowledge to Mr.Y.Kato of Kyoto University for his contribution on related wind tunnel tests in this research and Mr. S. Kusuhara of Honshu-Shikoku Bridge Expressway Company Limited for giving experimental data on AFM.

REFERENCES

[1] M. Matsumoto, Y. Nihara, Y. Kobayashi, H. Sato, H. Hamasaki: "Flutter mechanism and its Stabilization of Bluff Bodies", *Proc. of 9th ICWE*, pp827-838, 1995.

[2] M. Matsumoto, K. Okubo, Y. Ito, H. Matsumiya, G. Kim: "Branch characteristics of coupled flutter and its stabilization" *Proc. of 12th ICWE, Vol. 2*, pp2240-2246, 2007.

[3] A.Selberg: "Oscillation and aerodynamic stability of suspension bridges". *ACTA Plytechnica Scandinavica, Civil Engineering and Construction Series 13*, 1961.

[4] T. Miyata, K. Tada, H. Sato, H. Katsuchi, Y. Hikami: "New Findings of Coupled-Flutter in Full Model Wind Tunnel Tests of the Akashi Kaikyo Bridge", *Proc. of Symp. on Cable-Stayed and Suspension Bridges*, pp163-170, 1994.

[5] H. Sato, M. Kitagawa, T. Kanazaki, R. Toriumi, H. Katsuchi: "Wind Tunnel Test of the Akashi Kaikyo Bridge using Full Bridge Model", *Journal of Wind Engineering No.68*, pp25-36, 1996.

[6] Scanlan, R.H. and Tomko, J.J.: "Airfoil and Bridge Deck Flutter Derivatives", *Journal of Eng. Mech. Division, 97, EM6, American Society of Civil Engineering*, pp1717-1737, 1971.

[7] M. Matsumoto, H. Matsumiya, S. Fujiwara, Y. Ito: "On flutter fundamental modes, reduction of similar Selberg's formula and torsional divergence instability basing on SBSA" *6th BBAA*, 2008.